2020 NDIA GROUND VEHICLE SYSTEMS ENGINEERING AND TECHNOLOGY SYMPOSIUM
SURVIVABILITY TECHNICAL SESSION
AUGUST 11-13, 2020 - NOVI, MICHIGAN

An Easier Approach to Measuring Optical Distortion in Transparent Armor

James M. Gorman, PhD[1]

[1]US Army CCDC Ground Vehicle Systems Center, Warren, MI

ABSTRACT

Optical distortion measurements for transparent armor (TA) solutions are critical to ensure occupants can see what is happening outside a vehicle. Unfortunately, optically transparent materials often have poorer mechanical properties than their opaque counterparts which usually results in much thicker layups to provide the same level of protection. Current standards still call for the use of a double exposure method to manually compare the distortion of grid lines. This report presents provides a similar method of analysis with less user input using items typically available in many mechanics labs: machine vision cameras and digital image correlation software.

Citation: J. M. Gorman, "An Easier Approach to Measuring Optical Distortion in Transparent Armor", In *Proceedings of the Ground Vehicle Systems Engineering and Technology Symposium* (GVSETS), NDIA, Novi, MI, Aug. 11-13, 2020.

1. Introduction

Transparent materials are commonly used in vehicles because they provide a means for occupants to visually observe what is happening outside. In the automotive industry, research is being done into finding lower density materials to reduce overall vehicle weight, thereby increasing fuel economy [1]. Military vehicles face a similar weight problem, but their transparent solutions need to be able to withstand much more damage than is typically expected for a commercial vehicle. Unfortunately, glass and common optically transparent plastics have poor mechanical properties compared to their opaque counterparts. As a result, transparent armor (TA) solutions are inevitably thicker than comparable opaque solutions. This is one reason so much effort has been put into finding transparent armor solutions like spinel [2], which has much better properties than glass but with a greater processing/production cost.

Thicker TA solutions do more than just add mass to an already heavy vehicle: thick TA solutions increase the optical distortion. In a ground vehicle, highly-distorted TA may hinder the occupants' ability to determine if it is safe to dismount, select safe travel routes, or see threats. For fighter jets engaged in a dogfight, distortion may determine whether or not the threat is ended. As a result,

standards [3, 4, 5] have been written to quantify the amount of linear or angular distortion, and other specifications that will determine the acceptable amount of distortion for a given vehicle. These standards measure optical distortion by manually comparing the original and distorted images using the double-exposure method (whether using film or digital images).

A recent report [6] demonstrated three methods for measuring distortion: image comparison (double-exposure) method, Moiré Interferometry method, and Phase-Shifting Interferometry method. The standards [3, 4, 5] are all based off of the image comparison method. The authors [6] admit the phase-shifting interferometry method provides the highest resolution, but may be cost prohibitive and only useful for high-quality windows. The Moiré Interferometry method is relatively inexpensive and sensitive, but the experiments may be challenging. The method proposed here is an update to the image comparison method that remains relatively inexpensive, but removes some of the human measurement that can be time-consuming when many TA solutions are analyzed.

Over the last few decades, non-contact full-field measurement methods have become commonplace in mechanics and materials laboratories, with digital image correlation (DIC) [7] and the grid method [8] being the two most common techniques. While either method could be used, this report will focus on DIC.

Digital image correlation is a non-contact full-field displacement measurement technique [7]. The method works by using a non-uniform, semi-random pattern to track surface displacements. The two "flavors" of digital image correlation are 2D-DIC and 3D-DIC (also known as stereo-DIC). 2D-DIC uses one camera to measure displacements on nominally planar surfaces, with the camera situated perpendicular to the surface. Stereo-DIC uses two (or more) cameras to measure surface displacements, which allows users to measure displacements more accurately (due to camera triangulation), on non-planar surfaces, and account for out-of-plane displacement. While one might think 2D-DIC would be irrelevant now that machine-vision cameras are common and stereo-DIC software is commonplace, there are instances (such as scanning electron microscopy) where one is forced to use a single field of view. To increase the accuracy of 2D-DIC measurements, one can perform a calibration process on the camera similar to that used in stereo-DIC.

It should be noted that there are two general types of DIC algorithms: local and global [9]. Local, or subset-based, DIC splits the area of interest (AOI) to be analyzed into (many) smaller subsets that are tracked throughout the loading process. In contrast, global DIC works by analyzing the entire AOI at once (one large "subset"), similar to a finite-element calculation. Neither method works well for sharp discontinuities like edges or cracks, which led to the development of extended digital image correlation (X-DIC) [10]. This report will only consider local DIC, but global DIC could also be used.

While the raw displacement data output from DIC is useful by itself, experimenters often want to take the derivative of the displacements to back out the strains or rotations. This ability is one of the driving forces behind using DIC in material testing. For a uniaxial tensile test, this (full-field) strain data allows users to visually observe (instead of just assuming) the strain in a dog-bone specimen is uniform. Furthermore, the full-field displacement/ strain measurements have opened up new mechanical testing methods, such as the Virtual Fields Method [11, 12, 13], which uses *non-uniform* strain fields to back out multiple constitutive parameters during a single test.

In reference [14], the authors propose an automated method to measure optical distortion in aircraft transparencies using the standard grid board and then using a computer algorithm to analyze the distortion maps to determine whether or not the windshields are acceptable. The use of a computer algorithm to analyze the distortion (or *deformation*) a uniform pattern is essentially how the grid method analyzes surface deformation, as the grid method requires a uniform pattern.[1]

If one's goal is to measure how a pattern deforms, one does not need to follow the example of reference [14] and write one's own code. There are many commercial, university, or open-source DIC codes available. Reference [15] is a recent paper that compared many different codes analyzing the same images, and the author encourages the interested reader to begin there when considering different DIC software. If a laboratory is already using DIC, then it already has the DIC software and probably the necessary machine vision cameras typically used for DIC. Therefore, only a large semi-random speckle pattern is required to replace the grid board. The author suggests three general options for speckle patterns: the "optimized" DIC speckle pattern [16], using existing software to produce a pattern [17], or writing one's own code. After the pattern is generated, one will want to print out the pattern on a poster board or banner, whatever size is required to take the place of the grid board it is replacing. While one could in theory use aerosol paint or an airbrush to produce a semi-random pattern, the author expects users may save time by printing one off. However one produces a speckle pattern, the author emphasizes that matte paint or ink should be used to minimize the likelihood of over-saturating camera pixels.

There appears to be multiple methods of defining distortion. In Reference [14], the distortion is defined as the "relative magnification" or the divergence of the displacement field. With horizontal displacements u and vertical displacements v, this would result in distortion being defined as

$$D = \frac{du}{dx} + \frac{dv}{dy} = \varepsilon_{xx} + \varepsilon_{yy}, \quad (1)$$

where ε_{xx} and ε_{yy} are defined using the typical small strain approximation.[2] In Reference [18], the "line slope" is used as the determining factor. The former definition appears to use the sum of ε_{xx} and ε_{yy}, while the latter appears to use a measure of shear strain or rotation. Since this report is not intended to replace any standard or metric (but rather to demonstrate how DIC may be used to measure distortion), for comparison purposes this report will look at ε_{xy}. As DIC can just as easily export displacement, strain, or rotation data, any of these quantities could be used by DIC to evaluate distortion.

2. EXPERIMENTAL METHODS

The intent of this paper is to introduce an optical distortion measurement that is less manually intensive than current methods. As a result, the setup distances between the "grid board", "transparent part", and "camera" are identical to those described in the relevant standards [3, 4, 5]. One can see a picture of the setup in Figure 1, where the printed speckle pattern is covering the previously-used grid board.

It is beyond the scope of this report to give a thorough introduction to digital image correlation

[1] If one insists on continued use of the grid-board, one might be able to use the grid method to analyze such images. That said, the author would still suggest replacing the grid board with a poster of uniform pattern in order to no longer worry about strings that become limp and no longer perpendicular to each other.

[2] It should be noted that small "strains" are assumed throughout this report. If one is required to use a finite strain definition for accurate strain measurement, then the optical distortion is probably large enough to cause the TA to fail the vehicle's optical distortion standard.

and an exhaustive list of DIC tips and recommendations. That said, the author will provide some justification for choices made throughout this report, as deemed necessary. For interested readers, the author suggests references [7, 19, 20, 21, 22, 23] for additional background information on digital image correlation. For suggestions on using DIC, the author directs interested readers to the DIC Good Practices Guide [24], where one will find many tips, recommendations, and guidelines, along with citations of the original journal articles.

The strength behind DIC is its full-field imaging capability. Users can increase displacement accuracy by using larger subsets, but may lose fine aspects due to over-smoothing. For the data analyzed here, the DSLR camera (Canon EOS 7D with a zoom lens) used a subset size of 31 and a step size of 9. For the equivalent grid board measurement, the "step size" would be about 45 pixels. Therefore, by using DIC at these settings, the data was about 25 times as dense for DIC and the computer did all of the analysis. For the machine vision camera (Flir Blackfly with a 16 mm fixed focal length lens), a subset size of 16 and step size of 5 were used.

Since two different subset and step sizes were used, this difference ought to be justified. While the camera/lens combinations had approximately the same field of view, the DSLR camera captured 17.9 megapixels per image while the Flir machine vision camera only captured 5 megapixels. When measuring the dimensions of each pixel per camera, it was determined that one pixel in DSLR images was approximately half the length of one pixel in the machine vision image. Therefore, the subset and step sizes in the machine vision camera were reduced to approximately half that of the DSLR camera to account for this difference.

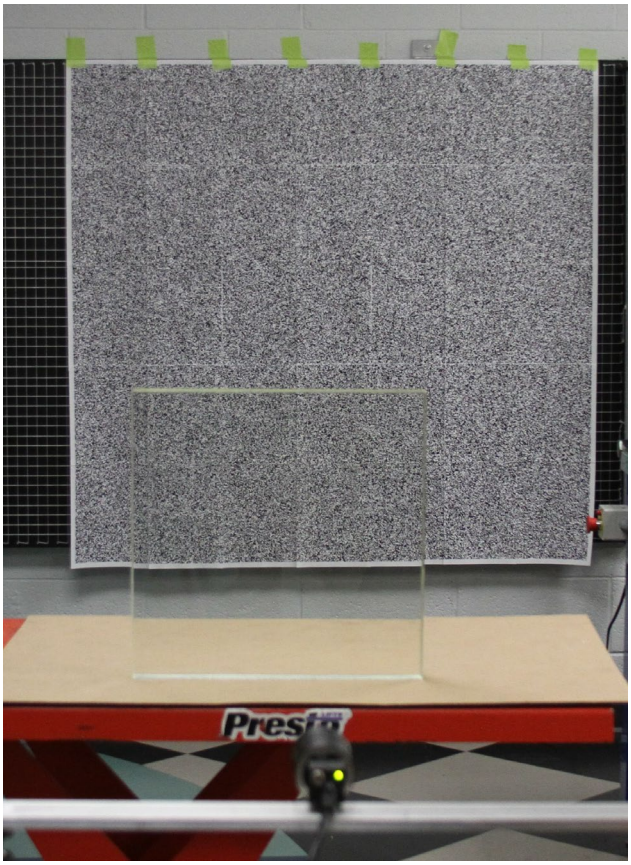

Figure 1: The experimental setup used to measure the distortion of the TA. As the reader can see, the only real difference in the setup between the standards [3, 4, 5] and the present case is the use of a printed speckle pattern instead of the grid lines.

In keeping with the guidelines of the aforementioned standards [3, 4, 5], a single camera was used to acquire images. When using 2D-DIC, one is reminded that the camera ought to be setup as perpendicular as possible to the DIC speckle pattern (the updated "grid board"). Camera lenses (and possibly extension tubes) should be chosen to maximize the TA part within the camera field of view. A machine vision camera ought to be used to decrease camera movement when images are taken, and a long-focal length lens should be attached to the camera[3] [24]. A comparison between a zoom

[3] In general, a telecentric lens is suggested for 2D-DIC [24]. However, the size of many TA layups to be analyzed (which can be on the order of a meter) makes producing and using such large telecentric lenses unrealistic.

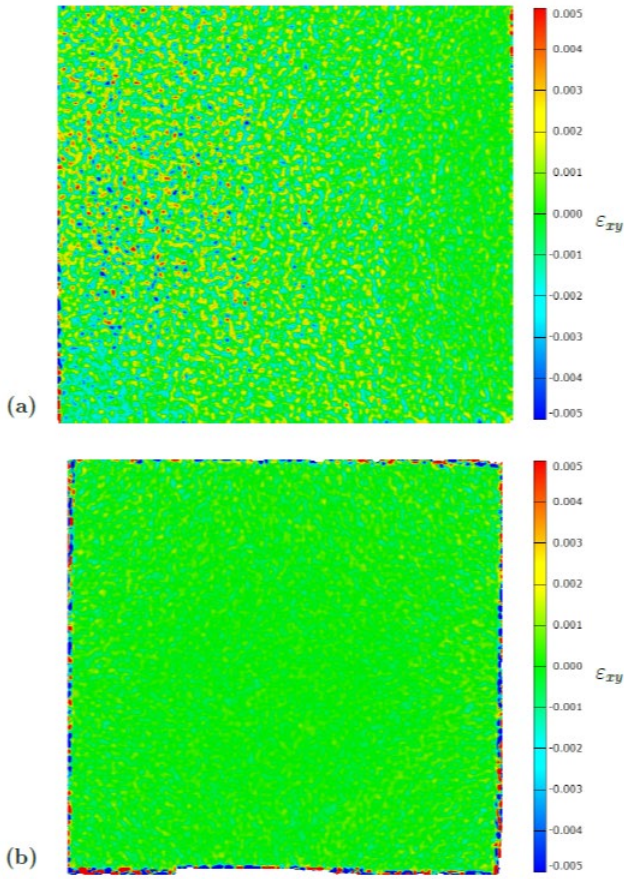

Figure 2: Comparison of **(a)** a DSLR camera with a zoom lens and a **(b)** machine vision camera with a long focal-length lens. The images analyzed were taken immediately following a reference image, which gives an estimate of the noise that may be present in the system. The DSLR camera is noisier than the machine vision camera. While ε_{xy} is used as an example, similar plots could be found for ε_{xx}, ε_{yy}, or rotation. The colormaps are capped at ±0.005 for comparison purposes. Note that (a) uses a subset size of 31 and step size of 9 while (b) uses a subset size of 16 and step size of 5. This was done to account for the different resolutions between the two cameras.

lens on a handheld camera and a fixed focal-length lens on a machine-vision camera is given in Figure 2.

The data in Figure 2 was calculated by taking two images back-to-back on the same camera and using the DIC software Aramis [25] to run the analysis for two different camera setups: a DSLR camera with a zoom lens and a machine vision camera with a fixed focal-length lens. It should be noted that the cameras were placed on tripods and not an optics table, nor was the lighting optimized for each camera individually (as each required different lighting needs). While Aramis allows users to run a calibration for 2D-DIC, this option was not utilized. The first image taken from each camera was used as a reference, while the second image (taken seconds after the first *with no TA layup present*) was used to estimate the level of noise for the camera and lens combination. As the two images are taken sequentially with no change between the two images, the measured displacements and strains should be zero.

As seen in Figure 2, the measured strains are not zero across the speckle pattern (the "grid board"). While a computer-generated random speckle pattern was used, the lighting between each camera was not optimized which may have resulted in degraded pixel matching. As the cameras were not mounted on an optical table, vibrations in the floor were likely present. The DSLR camera has the additional inherent motion in the camera each time an image is captured because a button was pressed on the camera for each image, although this could be ameliorated by using a remote image-capture signal. All of these contribute to image noise[4].

The noise level here appears to be low enough for measuring TA layups with respect to reference [18], where the line slopes must be below 5%. However, if less distortion is required, such as might be the case for aircraft or spacecraft, the current noise level might be too large. DIC may still

[4] DIC often correlates poorly around the outer edge of the area of interest (the region where deformation is measured). This can be seen on some of the edges in Figure 2. Some local DIC software packages do not correlate within a half-subset of the edge of the AOI for this reason. As a result, one often ignores results along the edge of the AOI unless one has reason to believe the results are real.

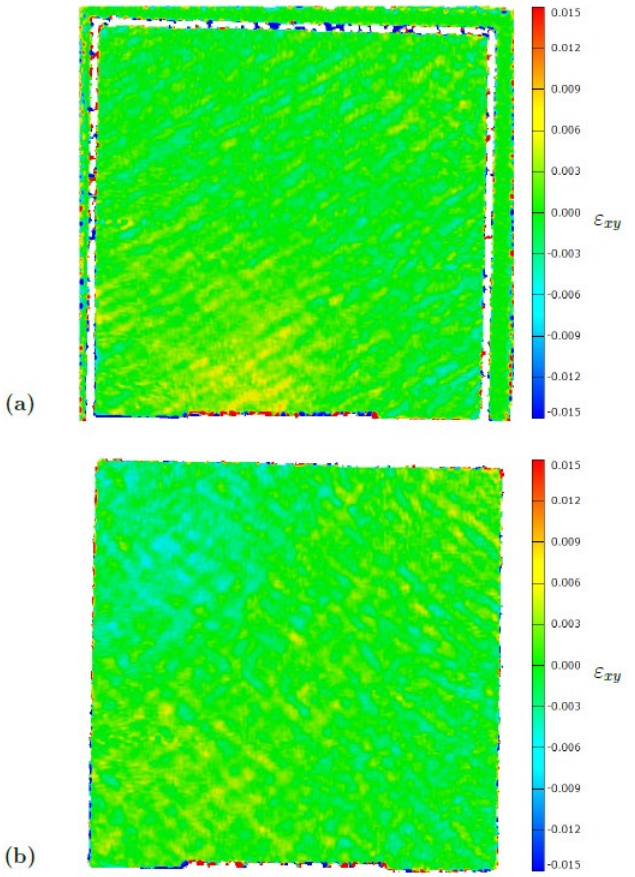

Figure 3: The distortion (here defined as the tensorial shear strain) maps above come from a generic TA layup containing **(a)** 3 panels of glass and **(b)** 4 panels of glass. While there does exist a fine structure to the shear strain across the TA, the distortion is rather small. In (a), one sees the outline of the TA layup where DIC was unable to correlate.

be a viable option to measure the distortion in those cases, but this might involve optimizing the speckle pattern, lighting, vibration dampening, *etc*. For tips on decreasing DIC noise, the interested readers are directed to the DIC Good Practices Guide [24].

3. TESTING

As mentioned above, this report uses the relevant standards [3, 4, 5] to measure the distortion, except that the grid board has been replaced by a speckle pattern and a generic 2D-DIC algorithm [25] has replaced human measurement. Method B/II is used here, with 300 cm between the speckle pattern and transparent part and 150 cm between the transparent part and camera(s). This shorter distance is more convenient to be used in smaller rooms. This same method may be used for Method A/I, but a different camera/lens combination will likely need to be used.

As a first measure of applicability, the distortion (tensorial shear strain) for two different layups will be considered: a generic 3-panel glass layup and a generic 4-panel glass layup. As the reader can see from the colormaps in Figure 3, both panels have relatively small distortion. In Figure 3a, one sees the outline of the TA panel where correlation was mostly lost along the edge.

These distortions are small enough that it would difficult to measure by hand; one might only be able to state that the panels passed because the distortion is below the failure threshold. In the case where a user would have to judge many TA layups, one could simply plot the distortion results as colormaps with the appropriate tolerance (say, ±5% of some strain measure), and then quickly flip through many plots to see whether each layup passes or fails.

Having demonstrated the applicability of distortion measurement on a TA layup with small distortions, now it is time to consider one with larger distortions. Figure 4 shows the distortion map for this final layup. As the reader can see, the distortion is much worse than the two considered previously.

The distortion in Figure 4 is so bad that it is worth considering the original images analyzed. The reference and deformed images can be found in Figure 5. The distortion is bad enough in this layup that one can visually see the blurring, although one does not expect the distortion to always be so apparent.

When using DIC, it has been noted that image correlation is often poor (or lost) close to edges or

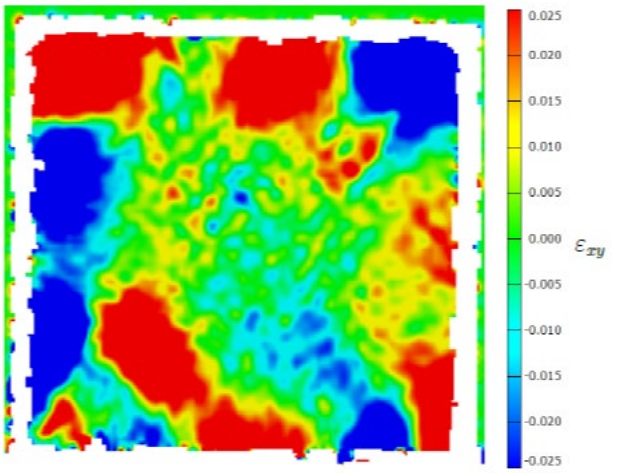

Figure 4: The final panel considered is a thicker panel than considered in Figure 4. Whereas the previous layups had relatively little distortion, this layup has much larger distortion. It should be noted that these colormaps were capped at ±0.025, and the colormap was cropped for clarity.

cracks. Therefore, when one is analyzing a field of view where the TA layup's edge is considered, one needs to be aware that artificially high (and unrealistic) strains or displacements may be present at boundaries as numerical artifacts. The user must be aware of this possibility. This is a reason to determine the maximum allowable distortion quantity: by setting the upper and lower bounds appropriately and plotting the colormaps (as done in Figures 3 and 4), one can quickly flip through many TA layups and determine whether each passes or fails. One could also write a computer program to do this, as done in reference [14]. Of course, the distortion at the TA boundaries may be able to be ignored [18], and the reader is encouraged to consult the relevant standards to answer this question.

It should be noted that the work here only demonstrated the ability of one to use digital image correlation to measure distortion (generically defined); not all of the specific aspects were considered. One aspect not considered until now is analyzing TA layups that are much larger than the camera's field of view. One option is to move the TA vertically and horizontally, taking enough

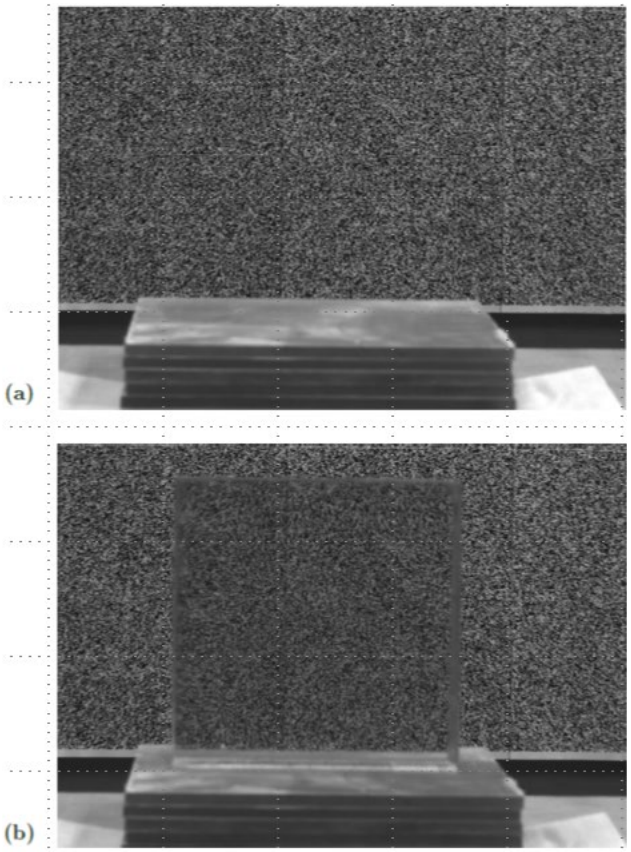

Figure 5: The **(a)** reference and **(b)** raw images used to determine the strains in Figure 4 (cropped for emphasis). One can tell from this raw image that the distortion in the panel is large, and it is questionable whether such a panel would be fielded.

images to cover the layup's entire area. Each of the images may be analyzed separately in DIC, and determine that each portion of the TA meets the distortion requirement. If each portion meets the requirement, then the entire TA layup would pass.

While this would be fine, some readers might want to combine the images/colormaps together into one conglomerate image. A word of caution must be emphasized if this is pursued. The two options for this approach would be to combine the images first and then run DIC analysis on the larger image [26], or to run DIC on the individual images and then combine the analyzed data together [27]. This latter approach ought to be used, and the tests should be run such that the DIC noise is minimized.

While there exist multiple reasons for this choice, the most important one is to remember the DIC has sub-pixel resolution. Other image software used to combine images may not have as high resolution, and one would artificially increase noise when combining images. This noise might increase the distortion enough to cause the conglomerate image to fail while the individual images passed.

4. FUTURE WORK

This work has focused on the use of 2D-DIC for analyzing optical distortion in order to follow the aforementioned standards. However, 3D-DIC (Stereo-DIC) is more accurate due to camera triangulation and preferred whenever possible. Future work will consider how 3D-DIC might be used to measure optical distortion of transparent armor.

5. CONCLUSIONS

This report updates the image-comparison method specified in standards [3, 4, 5] using readily-available digital image correlation software to decrease human measurement of optical distortion in transparent armor. Using full-field imaging allows one to increase the density of the distortion data while also automating image comparison. This method does require the use of digital image correlation software, but there are many commercial and open-source versions to choose from. Some of these may be found in reference [15]. While there is an investment of time and resources that is required, many laboratories already have the required software and simply need to exchange the grid board backdrop for a random speckle pattern.

6. ACKNOWLEDGMENTS

The author would like to thank Mr. Timothy Talladay for the original discussion that led to this report, Mr. David Witherspoon for assembling the transparent armor samples, and Dr. Thomas Meitzler for his helpful review.

7. REFERENCES

[1] Shea, S.B., “54.5 MPG and Beyond: Materials Lighten the Load for Fuel Economy,” https://www.energy.gov/articles/545-mpg-and-beyond-materials-lighten-load-fuel-economy. Accessed 23 December 2019.

[2] McCauley, J.W., and Patel, P. “Evaluation of IKTS Transparent Polycrystalline Magnesium Aluminate Spinel (MgAl2O4) for Armor and Infrared Dome/Window Applications,” *Army Research Laboratory*, March 2013. Report No. ARL-SR-262

[3] *ASTM F733-09*, Standard Practice for Optical Distortion and Deviation of Transparent Parts Using the Double-Exposure Method, 2014.

[4] *ASTM F2156-11*, Standard Test Method for Measuring Optical Distortion in Transparent Parts Using Grid Line Slope, 2011.

[5] *ASTM F2469-10*, Standard Test Method for Measuring Optical Angular Deviation of Transparent Parts Using the Double-Exposure Method, 2010.

[6] Youngquist, R.C., Nurge, M.A., and Skow, M. “A Comparison of Three Methods for Measuring Distortion in Optical Windows,” *National Aeronautics and Space Administration*, April 2015. Report No. NASA/TM-2015-218822.

[7] Sutton, M.A., Orteu, J.-J., and Schreier, H.W. *Image Correlation for Shape, Motion and Deformation Measurements*, Springer, 2009, ISBN 978-0-387-78746-6.

[8] Grédiac, M., Sur, F., and Blaysat, B. “The Grid Method for In-plane Displacement and Strain Measurement: A Review and Analysis,” *Strain*, vol. 52, no. 3, p. 205-243, 2016.

[9] Wang, B. and Pan, B. “Subset-based local vs. finite element-based global digital image correlation: A comparison study,” *Theoretical and Applied Mechanics Letters*, vol. 6, p. 200-208, 2016.

[10] Réthoré, J., Hild, F., and Roux, S. “From pictures to extended finite elements: extended

digital image correlation (X-DIC)," *Comptes Rendus Mécanique*, vol. 335, no. 3, p. 131-137, 2007.

[11] Grédiac, M. and Pierron, R. "Applying the Virtual Fields Method to the identification of elasto-plastic constitutive parameters," *International Journal of Plasticity*, vol. 22, no. 4, p. 602-627, 2006.

[12] Ross, M., Pierron, F., and Štamborská, M. "Application of the virtual fields method to large strain anisotropic plasticity," *International Journal of Solids and Structures*, vol. 39, no. 3, p. 217-226, 2016.

[13] Fletcher, L., Van-Blitterswyk, J., and Pierron, F. "A Novel Image-Based Inertial Impact Test (IBII) for the Transverse Properties of Composites at High Strain Rates," *Journal of Dynamic Behavior of Materials*, vol. 5, p. 65-92, 2018.

[14] Dixon, M., Glaubius, R., Freeman, P., Pless, R., Gleason, M. P., Thomas, M. M. and Smart, W. D. "Measuring Optical Distortion in Aircraft Transparencies: A Fully Automated System for Quantitative Evaluation," *Machine Vision and Applications*, vol. 22, p. 791-804, 2011.

[15] Reu, P.L., Toussaint, E., Jones, E., Bruck, H.A., Iadicola, M., Balcaen, R., Turner, D.Z., Siebert, T., Lava, P., and Simonsen, M. "DIC Challenge: Developing Images and Guidelines for Evaluating Accuracy and Resolution of 2D Analyses," *Experimental Mechanics*, vol. 58, p. 1067-1099, 2018.

[16] Bomarito, G.F., Hochhalter, J.D., Ruggles, T.J., and Cannon, A.H. "Increasing accuracy and precision of digital image correlation through pattern optimization," *Optics and Lasers in Engineering*, vol. 91, p. 73-85, 2017.

[17] Gorjup, D., Slavič, J., and Boltežar, M. speckle-pattern (v. 1.3.1). https://pypi.org/project/speckle-pattern/#_les

[18] *ATPD-2352T*, Purchase Description: Transparent Armor, 2013.

[19] Cheng, P., Sutton, M.A., Schreier, H.W., and McNeill, S.R. "Full-field Speckle Pattern Image Correlation with B-Spline Deformation Function," *Experimental Mechanics*, vol. 42, no. 3, p. 344-352, 2002.

[20] Orteu, J.-J. "3-D computer vision in experimental mechanics," *Optics and Lasers in Engineering*, vol. 47, p. 282-291, 2009.

[21] Mazzoleni, P., Matta, F., Zappa, E., Sutton, M.A., and Cigada, A. "Gaussian pre-filtering for uncertainty minimization in digital image correlation using numerically-designed speckle patterns," *Optics and Lasers in Engineering*, vol. 66, p. 19-33, 2015.

[22] Su, Y., Zhang, Q., Xu, X., and Gao, Z. "Quality assessment of speckle patterns for DIC by consideration of both systematic errors and random errors," *Optics and Lasers in Engineering*, vol. 86, p.132-142, 2016.

[23] Pierré, J.-E., Passieux, J.-C., Périé, J.-N., Buarin, F., and Robert, L. "Unstructured finite element-based digital image correlation with enhanced management of quadrature and lens distortions," *Optics and Lasers in Engineering*, vol. 77, p. 44-53, 2016.

[24] "A Good Practices Guide for Digital Image Correlation," *International Digital Image Correlation Society*, Jones, E.M.C. and Iadicola, M.A. (Eds), https://doi.org/10.32720/idics/gpg.ed1

[25] *Aramis* (version 6.3.0-9), User Documentation, GOM, 2013.

[26] Carroll, J., Abuzaid, W., Lambros, J., and Sehitoglu, H. "An experimental methodology to relate local strain to microstructural texture," *Review of Scientific Instruments*, vol. 81, p. 083703, 2010.

[27] Chen, Z., Lenthe, W., Stinville, J.C., Echlin, M., Pollock, T.M., and Daly, S. "High-Resolution Deformation Mapping Across Large Fields of View Using Scanning Electron Microscopy and Digital Image Correlation," *Experimental Mechanics*, vol. 58, no. 9, p. 1407-1421, 2018.